Formation of Strong Hydrogel–Porous Solid Interface via Double Network Principle

Takayuki Kurokawa, Hidemitsu Furukawa[†], Wei Wang[††], Yoshimi Tanaka, and Jian Ping Gong*

Department of Biological Sciences, Graduate School of Science, Hokkaido University, Sapporo 060-0810, Japan

[†] Current address: *Yamagata University, 4-3-16 Jonan, Yonezawa-shi Yamagata, 992-8510 Japan*

[††] Current address: *School of Stomatology, China Medical University, Shenyang, 110002, China*

---

* Corresponding author

E-mail: gong@mail.sci.hokudai.ac.jp, Tel & Fax: 81-11-706-2774

E-mail addresses of the other authors:

T. Kurokawa: kurokawa@sci.hokudai.ac.jp

H. Furukawa: furukawa@yz.yamagata-u.ac.jp

W. Wang: wwang@sci.hokudai.ac.jp

Y. Tanaka: ystanaka@mail.sci.hokudai.ac.jp

Abstract

A method for binding a tough double-network (DN) hydrogel and a porous solid *via* the double network principle is proposed. The effects of the pore size of the solids and the structure of the DN gel in the pores on the bonding strength are investigated by a peeling test. Porous solids with pore sizes of the order of several micrometers afford strong gel–substrate interfaces. Under optimized conditions, a bonding strength as high as ~1000 N/m was reached. The results obtained are compared with the strength of the bulk DN gel, and discussed in terms of double network principle at the bonding interface.

1. Introduction

Hydrogels are soft and wet materials with many specific features such as solute permeability[1], low surface sliding friction[2, 3], and antifouling properties[4–6]. Owing to these features, hydrogels can be used in many fields, such as tissue-like materials to prepare load-bearing implants in the human body, low-friction surfaces for industrial purposes, and antifouling coating materials for submerged surfaces in marine environments[7, 8]. However, conventional hydrogels have low mechanical strength, because of which they are not suitable for the aforementioned applications. Recent innovations in synthetic chemistry have significantly contributed to the improvement of the mechanical strength of gels, thereby increasing their applicability in various

fields[9–12]. We have invented a double network (DN) principle to synthesize extra-ordinarily tough hydrogels by introducing a double network structure in hydrogels[11]. DN gels with an extra-ordinarily toughness should consist of a tightly cross-linked rigid polyelectrolyte, such as poly(2-acrylamido-2-methylpropanesulfonic acid) (PAMPS), as the first network, and a sparsely cross-linked flexible neutral polymer, such as polyacrylamide (PAAm), as the second network. Furthermore, the second network, which is interpenetrated with the first network, should be more than 10 times higher in concentration than the first network. Despite their high water content (90 wt%), DN gels synthesized with such an optimized composition exhibit high elastic modulus (0.3-1.0 MPa), and high compressive fracture strengths, similar to natural cartilages (20 MPa)[11, 13]. The DN principle to synthesize the tough hydrogels was further applied to various polymer combinations, and tough DN gels with good biocompatibility[14–16], low sliding friction[17], and excellent wear resistance[18] have been synthesized.

The invention of the tough DN hydrogels will tremendously promote the application of the material to various applications, for example, as artificial cartilage tissue. At present, most of the artificial joints, such as a hip joint and a knee joint, are made only from *hard and dry* materials such as ceramics, ultra high molecular weight polyethylene (UHMWPE), and metals [19–21]. Owing to the hard and dry nature of the solid materials, these artificial joints are lack in ultra-low friction, distribution of loads, and absorption of impact energy, which are fundamental functions of the real articular joints. Taking the advantage of their *soft and wet* nature, mechanically tough DN gels with a low sliding friction resistance are excellent materials as artificial articular cartilage and meniscus tissues. To realize these applications, however, one of the

substantial obstacles to be solved is how to form a strong bonding between the soft and wet gel and the hard and dry solid. For example, as one of the possible clinical applications of DN gels, articular hip joints consist of DN gel membrane of several mm in thickness, as artificial cartilage, coated on artificial bones, such as hydroxyapatite, is presented. In this case, DN gels must bind strongly to hydroxyapatite for such a kind of application.

However, it is extremely difficult to bind a hydrogel strongly onto a solid surface with a glue, because of its high water content (usually more than 85–90 wt%) and low surface sliding friction coefficient (usually less than 10^{-3})[2]. Hence, it is necessary to develop a strategy to bond the tough DN gels to hard and dry solids. If one look at the actual load-bearing bio-tissue junction between a soft tissue and a hard tissue, for example, the junction between ligament and bone, it can be seen that ligament insertions occur by means of fibrocartilage, which is divided into non-calcified and calcified regions. The calcified fibrocartilage *interdigitates* with the underlying subchondral bone [22]. This interdigitating structure inspires us to engineer the DN gel and solid interface with a microstructure by increasing the contact area between the two materials of different elasticity.

In this study, we aim at engineering a strong interface between a DN gel and a porous solid by anchoring the DN gel in the porous solid, taking advantage of the DN principle. Figure 1 illustrates the procedure for formation of an anchoring interface between a piece of a tough DN gel sheet and a porous solid substrate. First, PAMPS gel, which is used to form the first network, is synthesized in the voids in the porous solid substrate (a). Then, the porous solid substrate containing the PAMPS gel is immersed in the pregel solution containing AAm, which is used to form the second network;

subsequently, the porous solid is brought in contact with the PAMPS gel sheet that is also soaked in the AAm solution (b). After second polymerization, the PAAm gel is simultaneously synthesized both in the porous solid and in the PAMPS sheet (c). Using this method, a continuous network of PAAm is formed in the porous solid and the PAMPS gel sheet. This method affords a DN structure both in the porous solid and in the gel sheet. Owing to the osmotic swelling pressure, the DN gel sheet was firmly anchored to the porous solid, and the bonding strength of the interface is investigated in terms of the peeling force per unit width of the gel sheet and compared with the fracture strength of the bulk DN gel in terms of a tearing force per unit width. Under optimized conditions, a gel-solid interface whose bonding strength is comparable to the fracture strength of the bulk DN gel is obtained.

2. Experimental Section

2.1. Characterization of porous solid substrates

Three types of porous solid substrates were used in this study: glass, polyethylene (Asahi Kasei Chemicals Corporation, Japan), and sponge. The porous glass and polyethylene substrates comprised glass and polyethylene particles of approximately the same size. Prior to use, the porous glass substrates were cleaned using 15% HCl and pure water. Polyethylene was treated with a surfactant to make its surface hydrophilic.

The microstructures of the porous solids were observed by scanning electron microscopy (SEM, Hitachi S4000). The porosity of these solids was measured by immersing them in water, and the actual volume of solids was estimated according to the Archimedes principle.

2.2. Synthesis of DN hydrogel

The DN hydrogel was synthesized via sequential network formation (two-step polymerization). The first step in this polymerization reaction involves the synthesis of the PAMPS gel by thermal polymerization. The monomer 2-acrylamido-2-methylpropane sulfonic acid (AMPS), (Toagosei Co. Ltd., Japan), cross-linker N,N′-methylenebisacrylamide (MBAA) (Tokyo Chemical Industry Co., Ltd.), and thermal initiator potassium persulfate (KPS) (Wako Pure Chemical Industries Ltd.) were mixed to obtain the prehydrogel solution. Argon gas was bubbled through the prehydrogel solution containing 1 M AMPS, 4 mol% MBAA, and 0.1 mol% KPS (mole percentages of MBAA and KPS were calculated with respect to the monomer concentration) for 30 min; then, the solution was injected into a reaction cell consisting of a pair of glass plates separated by a 2-mm-thick silicone rubber. The cell was heated at 60 °C for ~10 h in a water bath. Then, the PAMPS gel (first network) was immersed in an aqueous solution of 2 M AAm containing 0.1 mol% MBAA and 0.1 mol% KPS for 1 day until equilibrium was attained. By sandwiching the AAm containing PAMPS gel between two glass plates, and then heating the sample at 60 °C for 10 h, the second network (PAAm) was polymerized, and we obtained the DN gel. After polymerization, the PAMPS/PAAm DN gel was immersed in pure water for 1 week; during this period, the water was changed thrice to completely remove the unreacted materials. Details are

provided in the literature[11, 13]. Hereafter, the PAMPS/PAAm DN gels will be referred to as PAMPS-x_1-y_1-z_1/PAAm-x_2-y_2-z_2, where x_i, y_i , and z_i (i = 1, 2) are the concentrations of the monomer (M), MBAA (mol%), and KPS (mol%) used in synthesizing the i-th network, respectively.

2.3. Formation of gel–porous substrate interface

As shown in Figure 1, the gel–solid bonding is formed via the anchoring of DN to the porous solid via a DN structure formation. Porous glasses (thickness: 4 mm) with different pore sizes were immersed in a pregel solution with the prescribed concentration of AMPS, MBAA, and KPS for three days until the pores were filled with the pregel solution; then, the porous glasses were placed in a reaction cell consisting of a pair of glass plates separated by a 5-mm-thick silicone rubber membrane. The reaction cell contained a pregel solution in which the concentrations of AMPS, MBAA, and KPS were identical to those in the pregel solution used for immersing the substrates. The cell was heated at 60 °C for 10 h in a water bath. This process afforded the PAMPS gel in the pores of the glass substrates. Then, the porous glasses were removed from the reaction cell and immersed in a mixture of 2 M AAm, 0–0.1 mol% MBAA, and 0.01 mol% KPS for 3 days until equilibrium was attained. The PAMPS gel formed inside the pores of the glass substrate and on the surface of the substrate swelled after immersion in the aforementioned mixture. A slice of PAMPS gel (thickness: 3.8 mm) that was preswelled in the same mixture was placed on the porous glass substrate containing the PAMPS gel; then, the glass substrate was placed in a reaction cell consisting of a pair of glass plates separated by a silicone rubber membrane, which was 0.5 mm thinner than

the total thickness of the porous glass substrate and the gel. Then, the reaction cell was sealed and heated at 60 °C for 10 h in a water bath. After polymerization, the porous glass substrate to which the DN gel was adhered was immersed in pure water for 1 week, during which period the water was changed thrice for complete removal of the unreacted materials. Hereafter, the DN gel–glass substrate interfaces will be referred to as PAMPS-x_p-y_p-z_p// PAMPS-x_1-y_1-z_1/PAAm-x_2-y_2-z_2. Here, x_p, y_p, and z_p are the concentrations of AMPS (M), MBAA(mol%), and KPS (mol%), respectively, used for the synthesis of PAMPS in the porous substrates; x_1, y_1, and z_1 are the concentrations of AMPS (M), MBAA(mol%), and KPS (mol%), respectively, used for synthesizing the PAMPS gel sheet. Further, x_2, y_2, and z_2 are the concentrations of AAm (M), MBAA(mol%), and KPS (mol%), respectively, used for synthesizing the PAAm gel in the porous glass and in the PAMPS gel sheet. The interfaces between the DN gel and the other porous substrates were formed by a similar procedure.

2.4. Measurements

The bonding strength of the DN gel to the porous material was evaluated by peeling tests. In order to elucidate if the bonding strength is associated to the double network structure, we compare the bonding strength of the DN-solid interface with that of the bulk fracture strength of DN gel. The strength of the DN gel was evaluated by a tearing test. The peeling tests and tearing tests were performed using a tensile-compressive tester (Tensilon PTC-1310A, Orientec, Tokyo, Japan).

2.4.1. Tearing test for determining the toughness of DN gel

The tearing test was performed using a commercial test machine (Tensilon RTC-1150A, Orientec Co.). The gels were cut into a trousers-shape, which has the standardized JIS-K6252 1/2 sizes (thickness w = 4.6 mm; length L = 50 mm (initial notch length: 20 mm); width d = 7.5 mm), with a gel cutting machine (Dumb Bell co., Ltd.). The two arms of a test piece were cramped and the upper arm was pulled upward at constant velocity of 50 mm/min (the lower arm was fixed). The tearing force F was recorded. The toughness of the DN gel was characterized on the basis of the fracture-resistant force per unit width $g = F_{\mathrm{ave}} / w$, where F_{ave} is the average tearing resistance force at a steady-state tearing, and w is the length (in the present geometry, it is the thickness w = 4.6 mm of the sample) of the gel along the crack-front line. Detailed geometry for the test is shown in Figure 2 of reference [23]. It should be pointed out that in our tests, the sample is torn by pulling one of its arm, while its other arm is fixed; thus, g becomes equal to the fracture energy G, which is defined as the energy required to create a fracture surface of nominal unit area [23, 24].

2.4.2. Peeling test for determining the bonding strength

Figure 2(a) illustrates the geometry of the DN gel–substrate interface subjected to the peeling test. Here, w, v, and F represent the width of the peeled gel (w=5 mm), the constant peeling velocity (v=50 mm/min.), and the fracture resistant force, respectively.

The bonding strength is also characterized by $g = F_{ave}/w$, where F_{ave} is the average fracture-resistant force required to peel the gel off from the solid surface. Figure 2(b) shows the method of calculation of g. It should be noted that in the present case, the geometry of the interface makes accurate estimation of G difficult. This is because one of the fractured surfaces (solid) is fixed horizontally, and the crack front moves along its surface; the other fractured surface (gel) moves at an angle to the direction of the peeling force. Hence, g is used instead of the fracture energy G to analyze the bonding strength.

2.5. Statistic analysis

The experimental results are expressed as mean ± S.D. In figure 6 and 7, the effect of pore size was analyzed by one-way ANOVA followed by the Bonferroni test for post hoc multiple range comparisons. Statistic significant group difference was set as $p < 0.05$[25]. In the case of comparison between bulk DN gel and the other anchoring interface, the Dunnett test was applied with $p < 0.05$[26]. Furthermore, student's *t*-test was applied with $p < 0.05$ for comparing between porous glass substrates and porous polyethylene substrates with almost the same pore size.

3. Results and Discussion

Figure 3 shows the SEM images of the porous glass substrates with pores of various sizes. Here, the glass substrates are named "P-X," according to their nature,

where X corresponds to the diameter of the glass particles (μm) that make up the substrate. The pore size is directly proportional to the size of the particles that make up the substrates. Thus, the characteristic pore size in the substrate is determined by the particle size. Figure 4 shows the porosity of the glass substrates; this porosity is calculated from the ratio of the actual volume of solids to the nominal volume. The porosity of the substrates in this study is in the range of 35–40% and shows a slight decrease with an increase in the diameter of the particles.

The side view of the DN gel–solid interface is shown in Figure 5(a). The transparent upper portion represents the DN gel, while the white lower portion represents the porous glass substrate. In order to measure the peeling strength of the interface, the bonding DN gel was cut into 5-mm-wide strips from the disk-shaped porous substrate, as shown in Figure 5(b). A notch was made by cutting the specimen at the DN gel–solid interface. The porous solid was adhered onto the substrate holder of the tensile-compressive tester using glue, and one arm of the trouser-shaped gel was clamped to the tester, as shown in Figure 5(c). Peeling measurements was performed at a peeling velocity of 50 mm/min.

Figure 6 shows the value of g of the interface between the DN gels and glass substrates with different pore sizes. We first compared g for different substrates in their as-prepared states. There were significant differences between the bulk DN gel and the other anchoring interfaces by the Dunnett test. However, the g value of P-5 substrate was significantly higher than that of any other porous substrates by the Bonferroni test. After swelling, the length of the gels increased by 9.4%, g of P-5 in its swollen state decreased by approximately 30% that of P-5 in its as-prepared state; a similar tendency was observed in the case of the bulk DN gels after swelling. In P-16, P-100, and P-250,

there was no considerable change in *g* even after swelling by the student's *t*-test. These observations showed that DN formation depends on the pore size of the substrate, and a relatively high bonding strength was observed when using a suitable substrate such as P-5.

Figure 7 shows the *g* values observed for the interface between the DN gels and other porous materials such as polyethylene with different pore sizes ((I–III), #100 (I), #200 (II), and #800 (III)), melamine foam (IV), and polyurethane foam (V). The pore sizes of #100 (I), #200 (II), and #800 (III) are similar to those of P-40, P-100, and P-160, respectively. The DN gels strongly bonded to the aforementioned porous materials, as they did to the glass substrates. By comparing the results obtained for polyethylene (Figure 7) with those obtained for glass (Figures 6), we found that irrespective of the difference in their nature, bonding strengths between substrates with similar pore sizes did not show significant difference by the student's *t*-test. Thus, the bonding strength at the interface between the DN gel and the porous substrates strongly depends on the pore size of the substrates. The *g* value of the interface between melamine foam and the DN gel was higher than that at the interfaces in the case of polyurethane foam and polyethylene. This can be attributed to the soft and deformable nature of melamine foam, because of which the stress of mismatch at the interface between the free-swelling gel and the gel constrained in the porous solid was relaxed.

Figure 8 shows the effect of the cross-linker concentration used in the PAAm synthesis on *g* when the PAMPS structure is identical both in the porous substrates and the PAMPS gel sheet (1 M AMPS, 4 mol% MBAA, and 0.1 mol% KPS). The second step in the two-step polymerization reaction is performed using a constant amount of monomer (2 M AAm) and initiator (0.01 mol% KPS), while change the amount of the

cross-linker (0–0.1 mol% MBAA). In the case of DN gels, *g* decreases with an increase in the cross-linker concentration in PAAm; this result is in agreement with our previous results[27]. At the interface, *g* increases when the cross-linker concentration in PAAm is increased to 10^{-2} mol%. When the cross-linker concentration is constant, *g* at the interface becomes as high as that observed in the case of the bulk DN gel. If the cross-linker concentration in PAAm exceeds 10^{-2} mol%, both *g* at the interface and *g* of the bulk DN gel show a sharp decrease. This implies that the network structure at the interface is identical to that of the bulk DN gel if the cross-linker concentration exceeds 10^{-2} mol%.

We now explain why a high cross-linker concentration is essential to form an interface whose *g* value is comparable to that of the bulk DN gels. By carefully investigating the surface of the porous substrate containing the PAMPS gel, we find that the surface of the PAMS gels is very rough, probably owing to restricted free swelling in the aqueous AAm solution. This rough and modulated surface morphology prevents complete contact between the surface of the PAMPS gel and that of the flat PAMPS gel. In order to reduce the swelling of PAMPS in the porous substrate, we increase the cross-linker concentration in the PAMPS gel network in the pores of the glass substrate and maintain the cross-linker concentration in the PAMPS network in the gel sheet at 4 mol%. As shown in Figure 9, *g* increases with cross-linker concentration of PAMPS gel in the pores. At cross-linker concentrations of 8 and 12 mol%, *g* at the gel–substrate interface exceeds 1000 N/m, which is almost twice the value of *g* observed when the cross-linker concentrations are 2 and 4 mol%. It should be noted that the bulk DN gel has the highest *g* value when the PAMPS network was at a cross-linker concentration of 4 mol%. This implies that the optimal cross-linker concentration of the PAMPS network

is different for the DN gel–substrate interface and the bulk DN gel.

It should be noted that if the PAMPS gel had not been synthesized in the porous substrate and the interface was formed by simultaneously synthesizing the PAAm gel in the porous substrate and the PAMPS gel sheet, the strength of the interface (between the DN gel sheet and the porous substrate containing PAAm gel) would have been very low. This indicates that the DN structure in the pores plays an important role in increasing the strength of the gel–substrate interface, which can be understood from the toughening mechanism observed for the DN gels[28–33]. When a conventional gel that consist of a single-network is broken, only the polymer chains located at the tip of a crack are ruptured; a very small amount of energy (1–10 J/m^2 for a conventional gel) is required for this rupturing[34] is needed. On the contrary, when a DN gel suffers fracture, the wide range (~100 μm from the fractured surfaces) of the first brittle PAMPS network ruptures to form small clusters (of ~100 nm in size estimated [28]) first; the fracture energy G required for this rupture is very high. Further, clusters act as multifunctional cross-linkers of the ductile PAAm chains. As a result, a significant amount of energy (~ 1000 J/m^2 for a DN gel prepared under optimized conditions) is required for the fracture process. We consider that a similar fracture process occurs at the gel–substrate interface. Although only the PAAm network was a continuous phase across the interface, wide ranges of PAMPS networks in the DN gel both inside the pores of the substrate and on the surface of the substrate rupture to form into small clusters near the interface; as a result, the bonding strength increases considerably.

Furthermore, it should also be noted that for a nonporous substrate, particularly for one with a rough surface, the gel–substrate interface will be too weak to be measured by peeling tests. This indicates that an increase in the extent of interfacial contact is not

crucial for increasing the bonding strength. Instead, the anchoring effect, that is, the confinement of DN gel in the micropores, is responsible for the high bonding strength. Investigation of the fractured surfaces of the gel-solid interfaces revealed that the failure occurred not because of the disanchoring of the gel from the micropores but because of the rupture of the gel at the interface. This indicates that the anchoring strength is higher than the interface strength.

4. Conclusions

A strong interface between tough PAMPS/PAAm DN gels and various porous solid substrates is achieved by the anchoring of DN to the porous solid via a DN structure formation. It is found that the strength of the gel– substrate interface depends on the pore size of the solid substrates. Porous solids with pore sizes of the order of several micrometers afford strong gel–substrate interfaces. DN gels with a densely cross-linked (cross-linker concentration: 8–12 mol%) PAMPS network, in the pores exhibit the highest bonding strength. Under optimal conditions, the bonding strength between the gel and the substrate was comparable to the strength of the bulk DN gel.

Owing to the universal methodology to form bonding via anchoring of gel to porous solids, we believe that the results of this study will be useful in increasing the applicability of these strength DN gels, for example, these gels can be used in along with porous hydroxyapatite for producing artificial cartilages for artificial joints in which tough DN gel and hydroxyapatite serve as artificial cartilage and bone, respectively.

Acknowledgments

Porous polyethylene (Sunfine™ AQ) was provided by Asahi Kasei Chemicals Corporation, Japan. This study was supported by a Grant-in-Aid for the Specially Promoted Research (No. 18002002) from the Ministry of Education, Science, Sports and Culture of Japan.

References

1) Hirota N, Kumaki Y, Narita T, Gong JP, Osada Y. Effect of charge on protein diffusion in hydrogels. J Phys Chem B 2000; **104**（42）: 9898–9903.

2) Gong JP. Friction and lubrication of hydrogels—its richness and complexity. Soft Matter 2006; **2**: 544–552.

3) Gong JP, Kurokawa T, Narita T, Kagata G, Osada Y, Nishimura G, et al. Synthesis of hydrogels with extremely low surface friction. J Am Chem Soc 2001; **123**: 5582–5583.

4) Rasmussen K, Willemsen PR, Østgaard K. Barnacle Settlement on hydrogels. Biofouling 2002; **18**: 177–191.

5) Katsuyama Y, Kurokawa T, Kaneko T, Gong JP, Osada Y, Yotsukura N, et al. Inhibitory effects of hydrogels on the adhesion, germination and development of Laminaria angustata originated zoospores. Macromol Biosci 2002; **2**:163–169.

6) Murosaki T, Noguchi T, Kakugo A, Putra A, Kurokawa T, Furukawa H, et al. Antifouling activity of synthetic polymer gels against cyprids of the barnacle (Amphibalanus amphitrite) in vitro. Biofouling 2009; **25**(4): 313–320.

7) Bray JC, Merrill EW. Poly(vinyl alcohol) hydrogels for synthetic articular cartilage material. J Biomed Mater Res 1973; **7**(5): 431–443.

8) Oka M, Ushio K, Kumar P, Ikeuchi K, Hyon SH, Nakamura T, et al. Development of artificial articular cartilage. Proc Instn Mech Engrs, Part H: J Eng Medicine 2000; **214**: 59–68.

9) Okumura Y, Ito K. The Polyrotaxane Gel: A Topological gel by figure-of-eight cross-links. Adv Mater 2001; **13**: 485–487.

10) Haraguchi K, Takehisa T. Nanocomposite Hydrogels: A unique organic-inorganic network structure with extraordinary mechanical, optical, and swelling/de-swelling properties. Adv Mater 2002; **16**: 1120–1124.

11) Gong JP, Katsuyama Y, Kurokawa T, Osada Y. Double-network hydrogels with extremely high mechanical strength. Adv Mater 2003; **15**: 1155–1158.

12) Sakai T, Matsunaga T, Yamamoto Y, Ito C, Yoshida R, Suzuki S, et al. Design and fabrication of a high-strength hydrogel with ideally homogeneous network structure from tetrahedron-like macromonomers. Macromolecules 2008; **41**(14): 5379–5384.

13) Huang M, Furukawa H, Tanaka Y, Nakajima T, Osada Y, Gong JP. Importance of entanglement between first and second components in high-strength double network gels. Macromolecules 2007; **40**(18): 6658–6664.

14) Azuma C, Yasuda K, Tanabe Y, Taniguro H, Kanaya F, Nakayama A, et al. Biodegradation of high-toughness double network hydrogels as potential materials for artificial cartilage. J Biomed Mater Res A 2007; **81**(2): 373–380.

15) Tanabe Y, Yasuda K, Azuma C, Taniguro H, Onodera S, Suzuki A, et al. Biological responses of novel high-toughness double network hydrogels in muscle and the subcutaneous tissues. J Mater Sci: Mater in Med 2008; **19**(3): 1379–1387.

16) Yasuda K, Kitamura N, Gong JP, Arakaki K, Kwon HJ, Onodera S, et al. A ovel double-network hydrogel induces spontaneous articular cartilage regeneration *In Vivo* in a large osteochondral defect. Macromol Biosci 2008; published online.

17) Kaneko D, Tada T, Kurokawa T, Gong JP, Osada Y. Mechanically Strong Hydrogels with an Ultra Low Friction Coefficient. Adv Mater 2005; **17**: 535–538.

18) Yasuda K, Gong JP, Katsuyama Y, Nakayama A, Tanabe Y, Kondo E, et al. Biomechanical properties of high toughness double network hydrogels. Biomaterials 2005; **26**(21): 4468–4475.

19) Long M, Rack HJ, Titanium alloys in total joint replacement-a materials

science perspective. Biomaterials 1998; **19**: 1621-1639.

20) Piconi C, Burger W, Richter HG, Cittadini A, Maccauro G, Covacci V, Bruzzese N, Ricci GA. Marmo E, Y-TZP ceramics for artificial joint replacements. Biomaterials, 1998; **19**(16): 1489-1494.

21) Ohgushi H, Kotobuki N, Funaoka H, Machida H, Hirose M, Tanaka Y, Takakura Y, Tissue engineered ceramic artificial joint—ex vivo osteogenic differentiation of patient mesenchymal cells on total ankle joints for treatment of osteoarthritis, Biomaterials, 2005; **26**(22), 4654-466.

22) Messner K, Gao J. The menisci of the knee joint Anatomical and functional characteristics, and a rationale for clinical treatment. J Anat 1998; **193**: 161–178.

23) Tanaka T, Kuwabara R, Na YH, Kurokawa T, Gong JP, and Osada Y, Determination of Fracture Energy of Double Network HydrogGels. J. Phys. Chem.B 2005; **109**(23): 11559-11562.

24) Nakajima T, Furukawa H, Tanaka Y, Kurokawa T, Osada Y, Gong JP. True chemical structure of double network hydrogels. Macromolecules 2009; **42** (6): 2184-2189.

25) Neter J. Kutner M H, Nachtsheim C J, and Wasserman W, Applied Linear Statistical Models. McGraw-Hill, New York (1996).

26) Zar J H, Biostatistical Analysis. Prentice-Hall, Upper Saddle River, NJ (1999).

27) Tanaka Y, Kuwabara R, Na Y-H, Kurokawa T, Gong JP, Osada Y. Determination of fracture energy of double network hydroggels. J Phys Chem B 2005; **109**: 11559–11562.

28) Na Y-H, Tanaka Y, Kawauchi Y, Furukawa H, Sumiyoshi T, Gong JP, et al. Necking phenomenon of double-network gel. Macromolecules 2006; **39**: 4641–4645.

29) Webber R, Creton C, Brown HR, Gong JP. Large strain hysteresis and Mullins effect of tough double-network hydrogels. Macromolecules 2007; **40**: 2919–2927.

30) Brown HR. A model of the fracture of double network gels. Macromolecules 2007; 40: 3815–3818.

31) Tanaka Y. A local damage model for anomalous high toughness of double-network gels. Europhys Lett 2007; **78**: 56005(5pp).

32) Tanaka Y, Kawauchi Y, Kurokawa T, Furukawa H, Okajima T, Gong JP. Localized yielding around crack tips of double-network gels. Macromol Rapid Commun 2008; **29**: 1514–1520.

33) Yu QM, Tanaka Y, Furukawa H, Kurokawa T, Gong JP. Direct Observation of Damage Zone around Crack Tips in Double-Network Gels. Macromolecules, 2009, **42**: 3852-3855.

34) Lake GJ, Thomas AG. The strength of highly elastic materials. Proc R Soc London 1967; **300**: 108–119.

Figure captions

Figure 1. Schematic illustration of the formation of (DN) gel– porous solid bonding by anchoring the gel via a DN structure formation.

Figure 2. (a) Schematics of peeling test conducted on the gel–solid substrate interface, (b) Calculation of the peeling force per unit length. g , to detach the gel from the solid.

Figure 3. SEM images of glass substrates with different pore sizes.

Figure 4. Porosity of glass substrates with different pore sizes. Values are means ± SD.

Figure 5. Photographs of DN gel–porous glass substrate interface. (a) Side view of the interface, (b) Top view of the interface, (c) Peeling measurements of the bonding strength of the gel on the solid substrates.

Figure 6. Value of peeling force per unit length, g, for fracture of DN gel-glass interface of different pore sizes of glass. Left: in as-prepared states, right: after swelling in water. For comparison, fracture strength of bulk DN gels is also shown in the figure. Samples used: DN gel, PAMPS-1-4-0.1/PAAm-2-0.1-0.1; DN gel junction, PAMPS-1-4-0.1// PAMPS-1-4-0.1/PAAm-2-0.1-0.01. Values are means ± SD.

Figure 7. Peeling force per unit length, g, for fracture of DN gel-solid interface of various porous substrates: (I) polyethylene (#100), (II) polyethylene (#200), (III) polyethylene (#800), (IV) melamine foam, (V) polyurethane foam. The right-hand

column indicates the tearing force per unit length, *g*, of bulk DN gel. Samples used: DN gel, PAMPS-1-4-0.1/PAAm-2-0.1-0.1; interface, PAMPS-1-4-0.1// PAMPS-1-4-0.1/PAAm-2-0.1-0.01. Values are means ± SD.

Figure 8. Dependence of *g* on the cross-linker concentration in the second network, y_2. (○) *g* of the interface between the DN gels and the glass substrate (P-5). (□) *g* of the bulk DN gel. Samples used: DN gel, PAMPS-1-4-0.1/PAAm-2-y_2-0.1; interface, PAMPS-1-4-0.1// PAMPS-1-4-0.1/PAAm-2-y_2-0.1. Values are means ± SD.

Figure 9. Dependence of *g* on the cross-linker concentration of the first network in the porous substrates, y_p. (○) *g* of the interface between the DN gels and P-5; (□) *g* of bulk DN gel. Samples used: DN gel, PAMPS-1-4-0.1/PAAm-2-0.1-0.1; interface,: PAMPS-1-y_p-0.1// PAMPS-1-4-0.1/PAAm-2-0.1-0.1. Values are means ± SD.

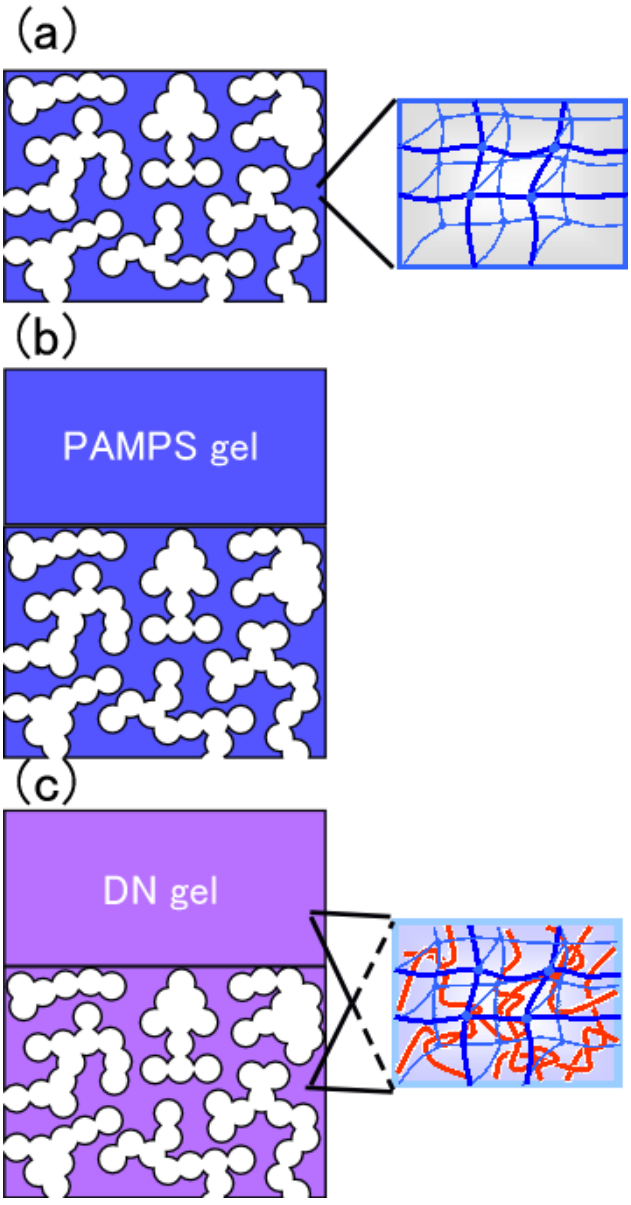

Figure 1. Kurokawa et al.

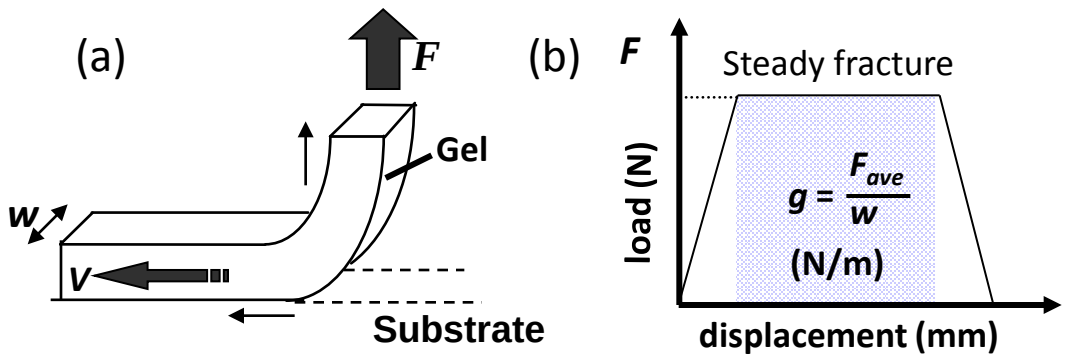

Figure 2. Kurokawa et al.

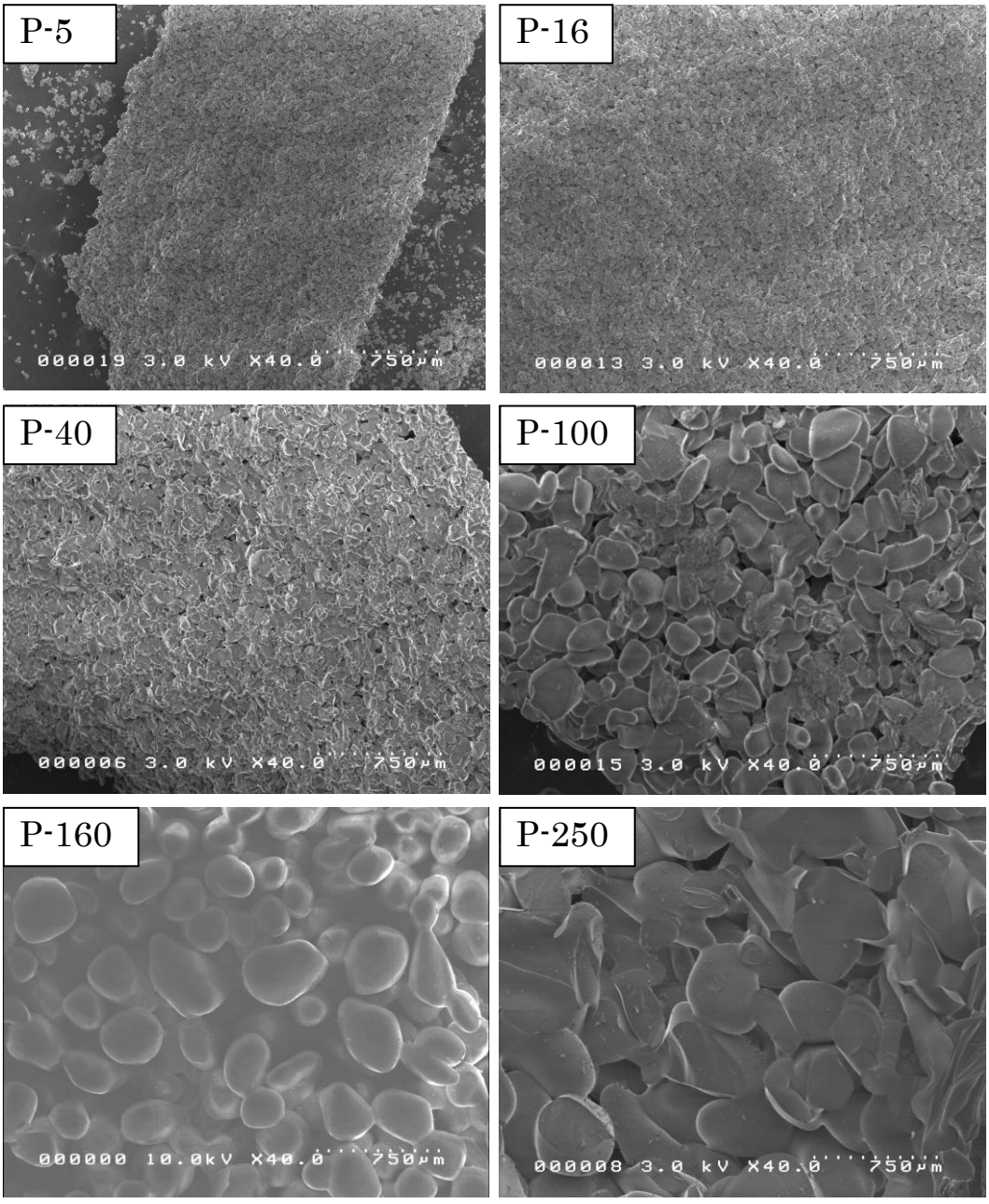

Figure 3. Kurokawa et al.

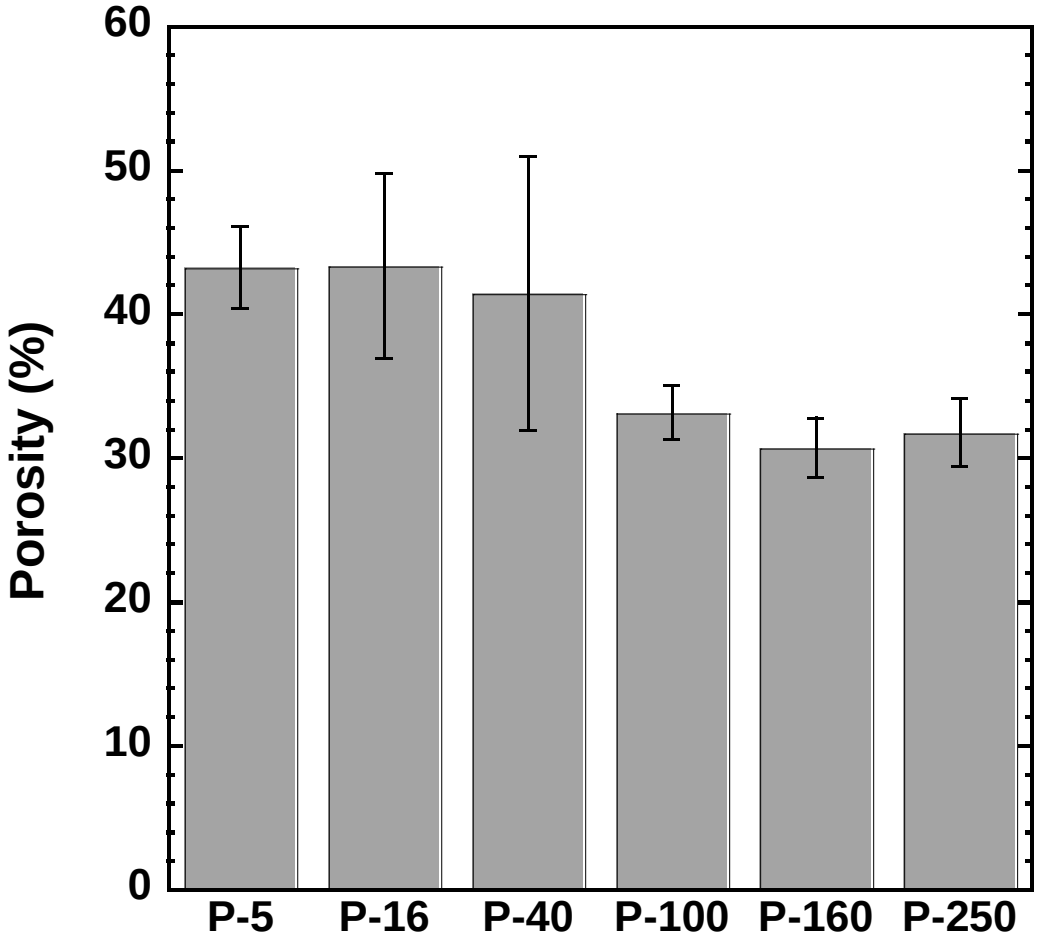

Figure 4. Kurokawa et al.

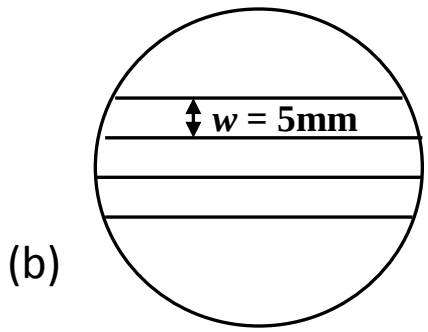

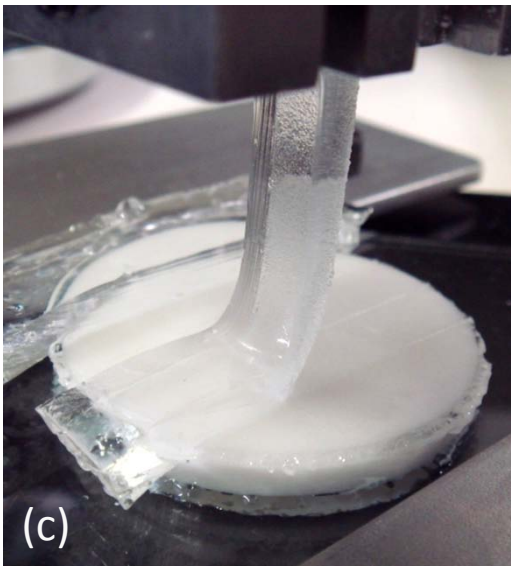

Figure 5. Kurokawa et al.

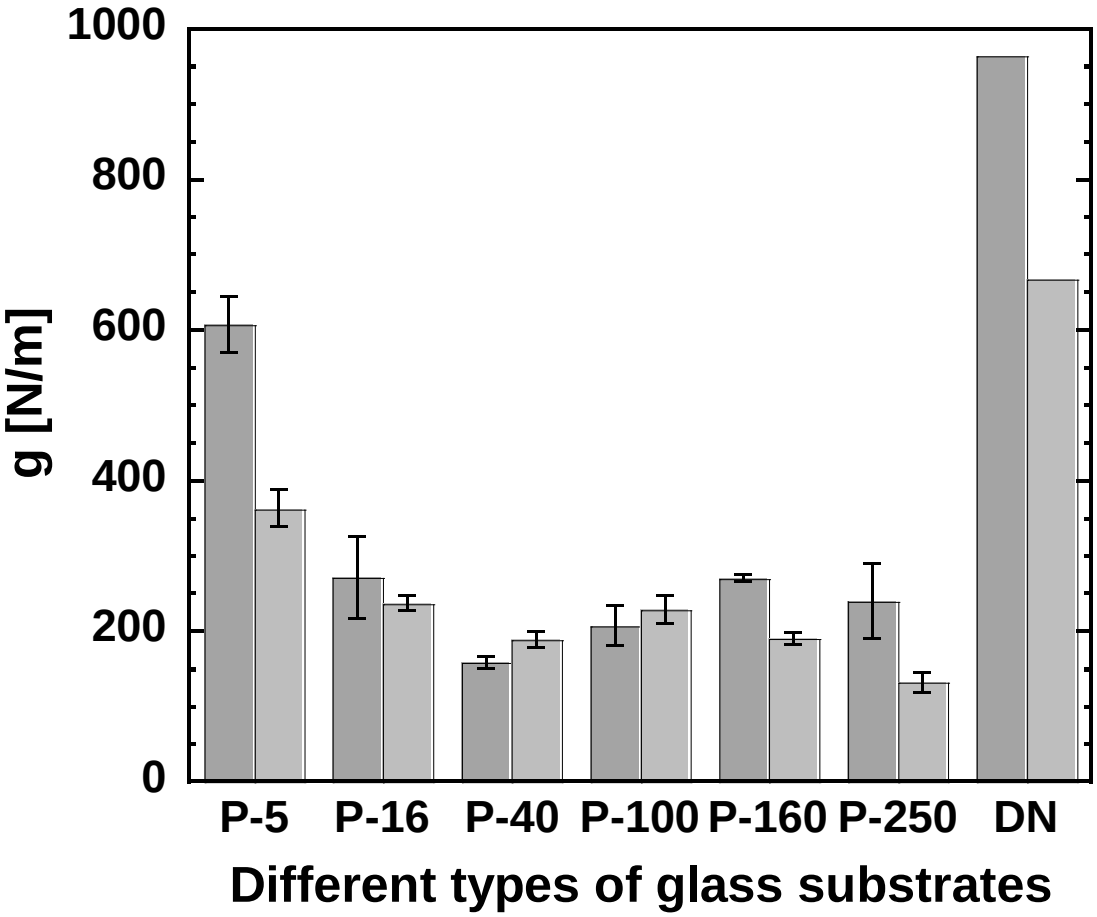

Figure 6. Kurokawa et al.

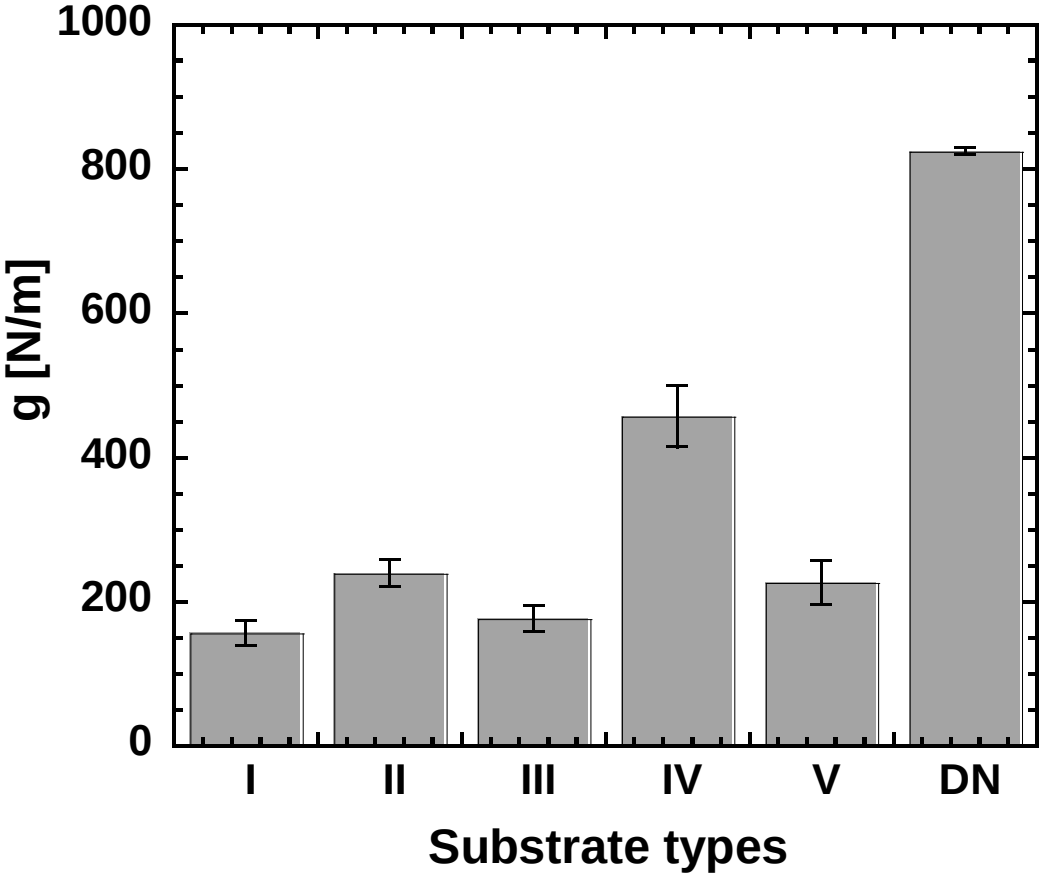

Figure 7. Kurokawa et al.

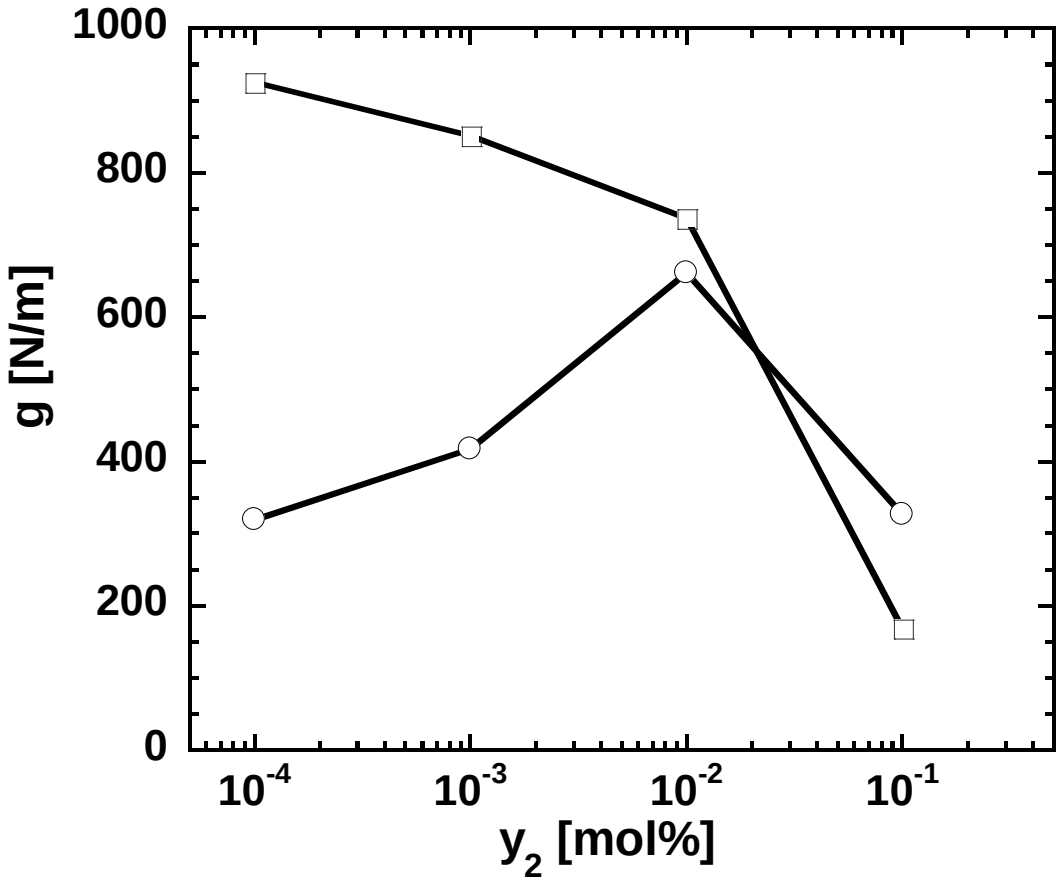

Figure 8. Kurokawa et al.

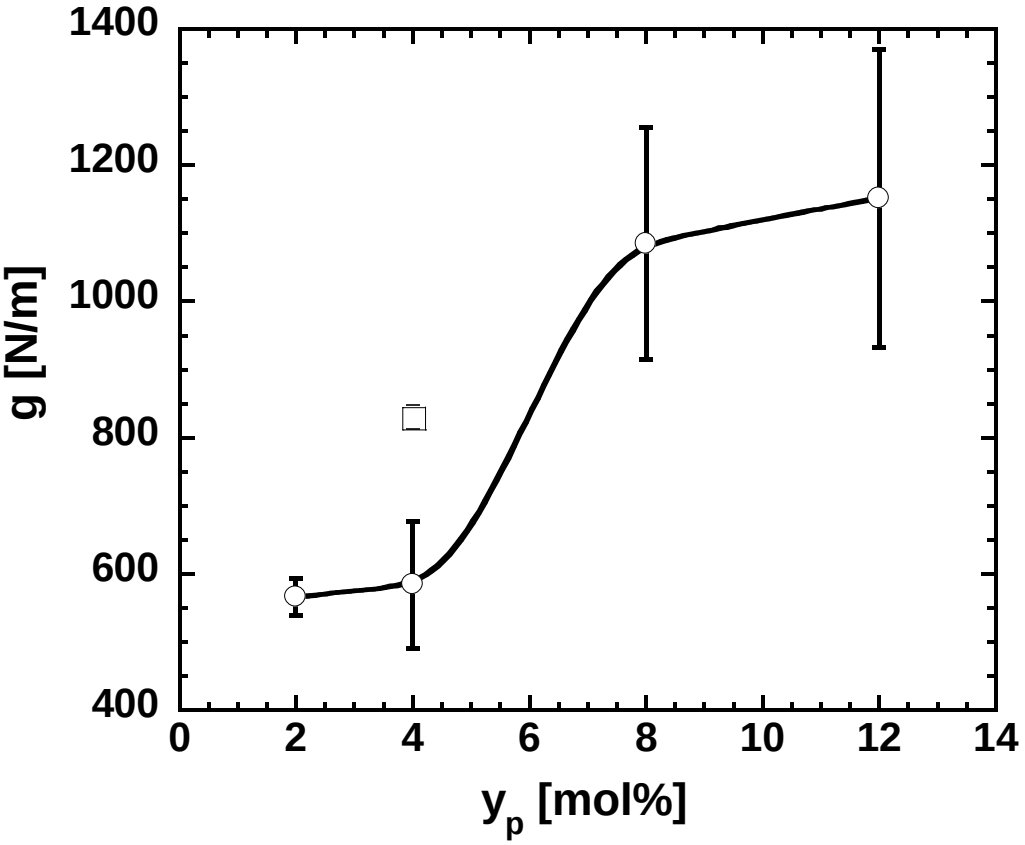

Figure 9. Kurokawa et al.